Nematic Phases in 1,2,4-Oxadiazole-Based Bent-Core Liquid Crystals: Is There a Ferroelectric Switching?

*Govindaswamy Shanker, Mamatha Nagaraj, Antoni Kocot, Jagdish K. Vij, Marko Prehm, and Carsten Tschierske**

Four series of new 1,2,4-oxadiazole derived bent-core liquid crystals incorporating one or two cyclohexane rings are synthesized and investigated by optical polarizing microscopy, differential scanning calorimetry (DSC), X-ray diffraction (XRD), electro-optical, and dielectric investigations. All the compounds exhibit wide ranges of nematic phases composed of tilted smectic (SmC-type) cybotactic clusters with strongly tilted aromatic cores (40–57°) and show a distinct peak in the current curves observed under a triangular wave field. Dielectric spectroscopy of aligned samples corroborates the previously proposed polar structure of the cybotactic clusters and the ferroelectric-like polar switching of these nematic phases. Hence, it is shown that this is a general feature of the nematic phases of structurally different 3,5-diphenyl-1,2,4-oxadiazole derivatives. In these uniaxial nematic phases there is appreciable local biaxiality and polar order in the cybotactic clusters. As a second point it is shown that electric field induced fan-like textures, as often observed for the nematic phases of bent-core liquid crystals, do not indicate the formation of a smectic phase, rather they represent special electro-convection patterns due to hydrodynamic instabilities.

1. Introduction

Liquid crystals (LCs) represent a fascinating state of matter[1] with wide technical applications in display industry[2] and optoelectronics,[3] significant importance for the development of new functional materials,[4] nanopatterning,[5] tissue engineering,[6] sensor and biosensor applications,[7] and also providing a fundamental concept in biological self-assembly.[8] This is due to the dual nature of LCs, combining features of anisotropic crystalline solids and isotropic liquids, enabling their soft self-assembled and ordered structures to respond to external stimuli, but also to their ability of self-healing of defects formed.[9] In recent years, chiral superstructures[10,11] and polar order[12] in the LC phases of achiral bent-core molecules have provoked interest of the researchers in this unique type of LCs.[13] Usually, in these bent-core mesogens 1,3-substituted benzenes, providing a 120° bent in the middle of the aromatic core, were used as bent units. However, also five-membered heterocycles, mainly 2,5-disubstituted 1,3,4-oxadiazoles leading to a bend of ≈134° have attracted significant attention (**1,3,4-Ox/(O)*n***, see **Scheme 1**).[14–18] The reduced bend (i.e., reduced deviation from linearity) of the aromatic core by the oxadiazole unit places these compounds at the borderline between classical rod-like LCs and the bent-core mesogens. Therefore, it can be expected that new types of LC phases combining features of both classes of LC could probably be observed with these materials.[19] One LC phase, considered as the "Holy Grail" in LC research is the illusive biaxial nematic phase (N_b).[20–23] Thermotropic biaxial nematic phases would not only be of fundamental scientific interest for soft matter physics, but also these phases are considered as possible candidates for next generation LC displays with enhanced switching performance.[24] There are simulations,[25,26] and also first experimental evidences that show induced and possibly spontaneous biaxiality could be generated in the nematic phases of oxadiazole based LCs.[15,18,27] In most oxadiazole-based bent-core LCs symmetric 2,5-disubstituted 1,3,4-oxadiazoles were used (**1,3,4-Ox/(O)*n***), whereas only few LC incorporate the slightly less bent (angle ≈ 140°) and non-symmetric 3,5-disubstituted 1,2,4-oxadiazole unit (**1,2,4-Ox/(O)*n***, Scheme 1).[28–30] Interest in LCs based on 1,2,4-oxadiazoles arose recently, as evidence of ferroelectric switching and induced biaxiality were reported for a nematic phase formed by one of these molecules (**1,2,4-Ox/O9**).[31] However, further experimental evidence is required to corroborate a ferro-nematic phase[32] and to develop general rules for molecular design of such materials.

The aim of this manuscript is threefold. First, a broader range of nematic 1,2,4-oxadiazoles incorporating one or two *trans*-4-alkyl substituted cyclohexane ring(s) in the core structure[15f,33,30] with symmetric and non-symmetric

Dr. G. Shanker, Dr. M. Prehm, Prof. C. Tschierske
Institute of Chemistry, Organic Chemistry
Martin Luther University Halle-Wittenberg
Kurt-Mothes-Str. 2, 06120 Halle, Germany
E-mail: carsten.tschierske@chemie.uni-halle.de
Dr. M. Nagaraj, Prof. A. Kocot, Prof. J. K. Vij
Department of Electronic and Electrical Engineering
Trinity College
University of Dublin
Dublin 2, Ireland
Prof. A. Kocot
Institute of Physics
University of Silesia
Katowice, Poland

DOI: 10.1002/adfm.201101770

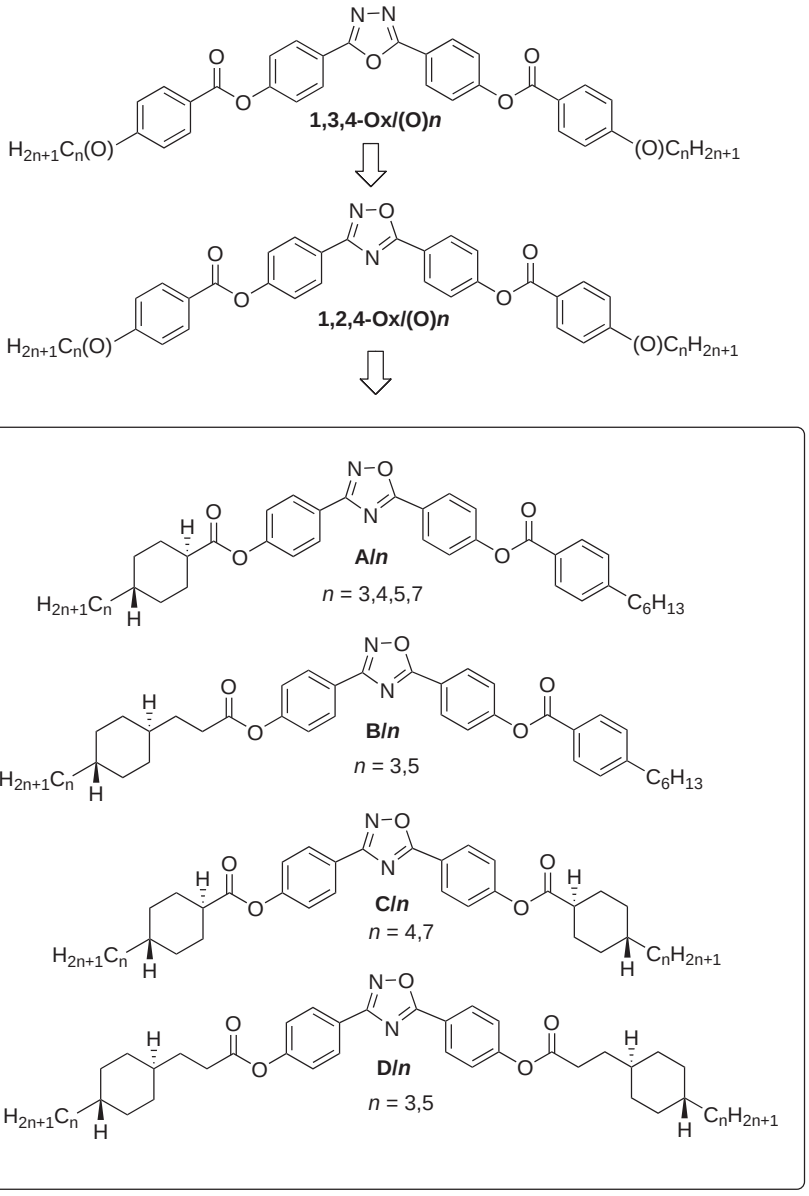

Scheme 1. Structure of previously reported bent-core 1,3,4-oxadiazoles (**1,3,4-Ox/(O)*n***)[31] and 1,2,4-oxadiazoles (**1,2,4-Ox/(O)*n***)[15] and the cyclohexane-containing 1,2,4-oxadiazoles **A/*n*** - **D/*n*** reported herein.

substitution patterns and different chain lengths (compounds ***A/n*-*D/n***, Scheme 1) are synthesized and investigated.

Secondly, it is found that the nematic phases of all synthesized compounds behave similar to the related benzoate **1,2,4-Ox/O9** reported previously[31] by showing a distinct current peak under a triangular wave voltage. This indicates that the current peak is a specific feature of the nematic phases of a broad range of structurally different 3,5-diphenyl-1,2,4-oxadiazoles. Temperature-, frequency- and cell-gap-dependence of the current peak intensity are in line with polar switching, which is further confirmed by dielectric investigations of aligned samples. In this way ferroelectric-like polar switching of these nematic phases is corroborated.

Finally, it is shown that the often observed field induced formation of fan-textures in the nematic phases of bent-core mesogens[34] is not necessarily an indication of the field induced formation of a smectic phase; rather these textures appear to represent special electro-convection patterns in most cases.

2. Results and Discussion

2.1. Synthesis

We have recently developed a simple and straightforward synthetic strategy to the non-symmetrically functionalized 1,2,4-oxadiazole based building block **1**,[35] which was used as starting material for the synthesis of the non-symmetrically substituted compounds ***A/n*** and ***B/n*** (**Scheme 2**). These compounds were obtained by acylation of **1** with *trans*-4-alkylcyclohexane carboxylic acid (Merck) or 3-(*trans*- 4-alkylcyclohexyl)propionic acid using dicyclohexylcarbodiimide (DCC) as condensation agent.[35]

For the synthesis of symmetric oxadiazoles ***C/n*** and ***D/n*** (**Scheme 3**), 4-benzyloxybenzoic acid **3** was treated with the amidoxime **2**, to obtain the benzyl protected phenol **4**, followed by debenzylation using 10% Pd/C in THF: EtOAc (3:7) for 7 h at 80 kPa to obtain the key intermediate 4,4′-(1,2,4-oxadiazole-3,5-diyl)biphenol (**5**).[29c] Bent-core molecules of series ***C/n*** and ***D/n*** were achieved by treating **5** with two equivalents of the corresponding carboxylic acids using DCC as coupling reagent.[36] All compounds were purified by column chromatography and probed for their molecular structure by spectroscopic methods and microanalytic techniques. Detailed procedures and analytical data of compounds ***C/n*** and ***D/n*** are collated in the SI, those of compounds ***A/n*** and ***B/n*** have been reported previously.[35]

2.2. Investigations

The obtained compounds were investigated by polarizing microscopy (Optiphot 2, Nikon) in conjunction with a heating stage (FP82HT, Mettler) and by differential scanning calorimetry (DSC) using a DSC-7 (Perkin Elmer). The assignment of the mesophases was made on combined results of optical textures and X-ray diffraction (XRD). Investigations on oriented samples were performed using a 2D detector (Hi-Star, Siemens AG). Uniform orientation was achieved in most cases by alignment in a magnetic field ($B \approx 1$ T) using thin capillaries. This orientation is maintained by slow cooling (0.1 K min^{-1}) in the presence

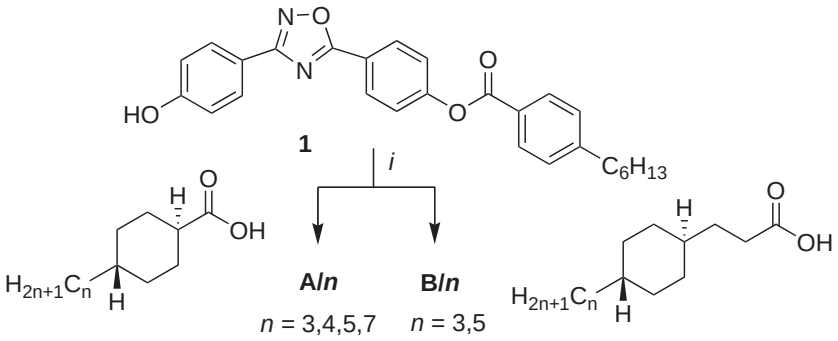

Scheme 2. Synthesis of compounds ***A/n*** and ***B/n*** incorporating one cyclohexane ring. Reagents and conditions: i) DCC, DMAP, CH_2Cl_2, 12 h, (65–70%).[35]

of the magnetic field. Due to the high transition temperature, compound **C/7** could not be aligned in the magnetic oven. This compound was aligned by slow cooling a drop of the sample on a glass surface and the X-ray beam was applied parallel to the surface. Electro-optical experiments have been carried out using a home built electro-optical setup in commercially available indium tin oxide (ITO) coated glass cells (E.H.C., Japan) with an antiparallel rubbed polyimide coating and measuring area of 1 cm^2. Dielectric investigations were performed using a Novocontrol Alpha high resolution dielectric analyser (Novocontrol GmbH, Germany). Uniform homeotropic orientation was achieved by alignment in a magnetic field (B = 1.2 T). The real and imaginary parts of the complex permittivity were measured in the frequency range of 1 Hz to 10 MHz, in a planar cell of 15 µm thickness, on slow cooling of the sample. The measuring voltage was 0.1 V_{pp}.

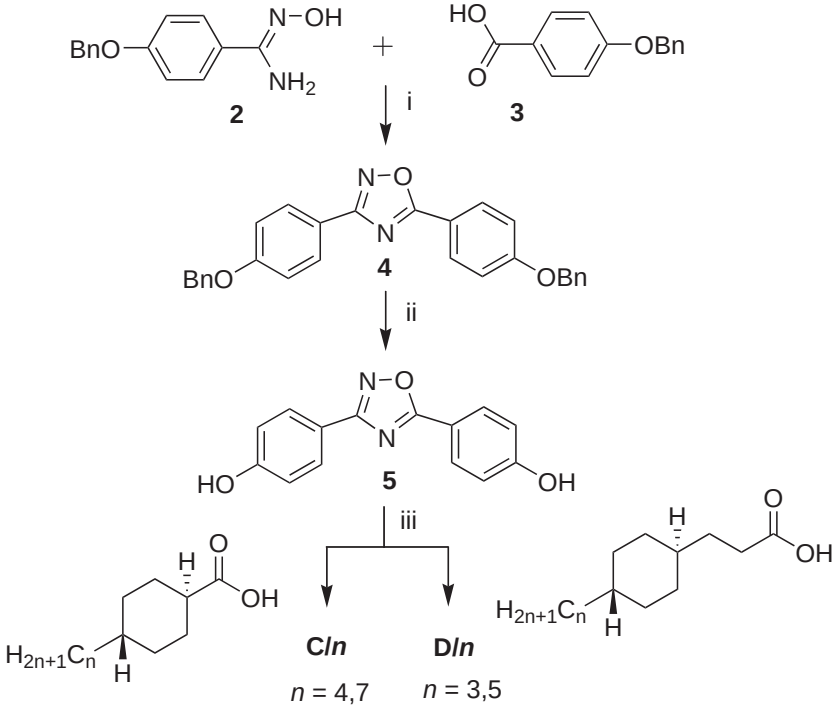

Scheme 3. Synthesis of compounds ***C/n*** and ***D/n*** incorporating two cyclohexane rings. Reagents and conditions: i) DCC, 1,4-dioxane, reflux, 8 h, (78%); ii) THF: EtOAc (3:7), 10% Pd/C, 80 kPa, 7 h (68%); iii) DCC, DMAP, CH_2Cl_2, 12 h, (64–69%).

2.3. Thermal Behavior of Compounds A/*n*-D/*n*

It is apparent from **Table 1** and **2** that all synthesized compounds display enantiotropic liquid crystalline phases. Particularly, they exhibit broad regions of nematic phases, which were observed down to the crystallization temperature for most of them. DSC traces of two selected compounds are shown in **Figure 1**. Only for the two compounds with the longest aliphatic segments, compounds **C/7** and **D/5**, additional SmC phases were observed. Though compounds **C/7** and **D/5** have the same total size of the aliphatic segments the SmC phase stability is reduced if the cyclohexane rings are shifted more to the periphery in the 3-(4-alkylcyclohexyl)propionate **D/5**. On the other hand the clearing temperatures of all 3-(4-alkylcyclohexyl) propionates ***B/n*** and ***D/n*** are significantly reduced compared to the corresponding 4-alkylcyclohexane carboxylates ***A/n*** and ***C/n***, most probably due to the increased flexibility of the propionate linking units compared to the shorter and more rigid carboxyl groups. Though there is a strong effect of this linking unit on the mesophase stability, reducing the clearing temperature by about 40–50 K for each of these units, there is no such effect on the melting temperatures. Therefore, the mesomorphic temperature ranges are smaller for the 3-(4-alkylcyclohexyl) propionates ***B/n*** and ***D/n*** compared to the 4-alkylcyclohexane carboxylates ***A/n*** and ***C/n***, respectively (see Table 1 and 2).

Upon cooling from the isotropic liquid state, the nematic phases (N) appear as droplets (**Figure 2**a) which coalesce to form Schlieren textures as shown in Figure 2b for the texture of compound **A/4** as an example. For compound **C/7** with an additional tilted smectic (SmC) phase, on cooling the nematic phase to 173 °C, the transition N-SmC (Figure 2c,f) takes place, which is seen in the homogeneously aligned nematic phase as formation of a fan-like texture. The nematic phases of all compounds are rather fluid, similar to the nematic phases of low molecular weight rod-like molecules and more fluid than usually observed for the nematic phases of other bent-core molecules.[41]

2.4. XRD Investigations

XRD measurements were performed for one representative from each series of compounds and the results are summarized in **Table 3**. Alignment of the samples of most compounds was achieved in the nematic phase under a magnetic field of medium strength ($B \approx 1$ T).

Table 1. Phase transition temperatures (T in °C), associated enthalpy values (in square brackets, ΔH in kJ mol^{-1}), and crystallization temperatures (T_{cr} in °C) of compounds **A/*n*** and **B/*n***.[a)]

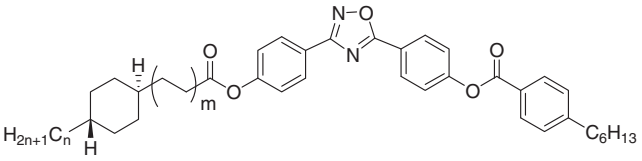

Compd.	*m*	*n*	Phase transitions	T_{cr}
A/3	0	3	Cr 149 [30.3] N 305 [1.5] Iso	85
A/4	0	4	Cr 120 [37.6] N 293 [1.4] Iso	95
A/5	0	5	Cr 129 [33.1] N 296 [1.1] Iso	112
A/7	0	7	Cr 124 [40.0] N 283 [1.1] Iso	98
B/3	1	3	Cr 127 [30.1] N 250 [2.0] Iso	100
B/5	1	5	Cr 123 [30.0] N 245 [1.5] Iso	99

[a)] Peak temperatures in the DSC thermograms obtained during the first heating cycles (phase transitions) and cooling cycles (T_{cr}) at 10 K min^{-1}. Abbreviations: Cr = crystalline solid; N = nematic phase; all nematic phases are composed of polar (P) SmC type cybotactic clusters (cybC) and hence represent N_{cybCP} phases; and Iso = isotropic liquid.

The XRD patterns observed for a magnetically aligned sample of compound **D/5**, as representative example, in the nematic and the SmC phase are shown in **Figure 3**. In the nematic phase at $T = 150$ °C, there are diffuse wide angle maxima at $d = 0.49$ nm, corresponding to the mean lateral distance between the molecules, indicating a fluid LC phase. The wide angle scattering are centred on the equator (Figure 3a) which indicates that the alignment of the bent-core molecules is along the long molecular axis.

The small angle scattering has its maximum at $d = 3.8$ nm which is a bit smaller than the molecular length ($L_{mol} = 4.2$ nm in a V-shaped conformation with a bending angle of 140° and all-*trans* alkyl chains, see Table 3). The intensity of the small angle scattering is significantly higher than the wide-angle scattering (Figure 3e), indicating a cybotactic nematic phase composed of relatively large clusters.[37,41] The small angle scattering is characterized by four diffused spots with clear maxima beside the meridian and smeared out to two dumbbell shaped streaks parallel to the equator (see Figure 3b), indicating that the cybotactic nematic phase is formed by SmC-like clusters (N_{cybC} phase).

The correlation length, estimated according to $\xi_{\parallel,\perp} = 2/\Delta q$ from the full width at half maximum (Δq)[38] in transversal direction is $\xi_{\parallel} = 8$ nm and in longitudinal direction it is $\xi_{\perp} = 2$ nm. The dimensions of the cybotactic clusters ($L_{\parallel,\perp}$) can be approximated to $L_{\parallel,\perp} = 3\xi_{\parallel,\perp}$,[39] leading to the values $L_{\parallel} = 24$ nm and $L_{\perp} = 6$ nm. Accordingly, the clusters are relatively large, composed on average of about 6 layers and about 12 molecules are arranged in the cross section.[40] A bit smaller values were obtained for the compounds **A/4** and **B/5** with only one cyclohaxane ring and without SmC phase, for which $L_{\parallel}$ is around 7 nm and $L_{\perp}$ about 3 nm, corresponding to about two layers and a lateral dimension of the clusters of about 6 molecules. In the nematic phase of compound **D/5** the splitting of the maxima of the small angle scatterings $\Delta\chi/2$ is about 36°, as the clusters are relatively large this splitting can be interpreted as the average tilt of the molecules in the SmC clusters (XRD-tilt).[34b,41,42] Very similar XRD patterns were recorded for the nematic phases of the other investigated compounds (see Figure S1–S3 in the Supporting Information). The $\Delta\chi/2$ splitting is very large for compounds

Table 2. Phase transition temperatures (T in °C), associated enthalpy values (in square brackets, ΔH in kJ mol^{-1}), and crystallization temperatures (T_{cr} in °C) of compounds **C/*n*** and **D/*n***.[a)]

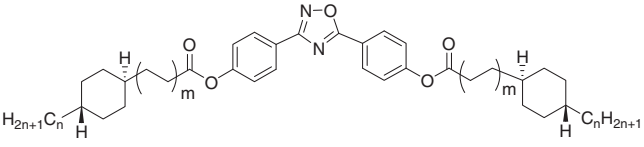

Compd.	*m*	*n*	Phase transitions	T_{cr}
C/4	0	4	Cr 157 [16.8] N 323 [1.6] Iso	138
C/7	0	7	Cr_1 82 [22.8] Cr_2 127 [16.2] SmC 173 [<0.01] N 282 [1.9] Iso	110
D/3	1	3	Cr 130 [26.7] N 229 [1.6] Iso	106
D/5	1	5	Cr 128 [23.0] SmC 131 [0.3] N 224 [2.4] Iso	111

[a)] Abbreviations: SmC = Smectic C phase. For other abbreviations see footnote of Table 1.

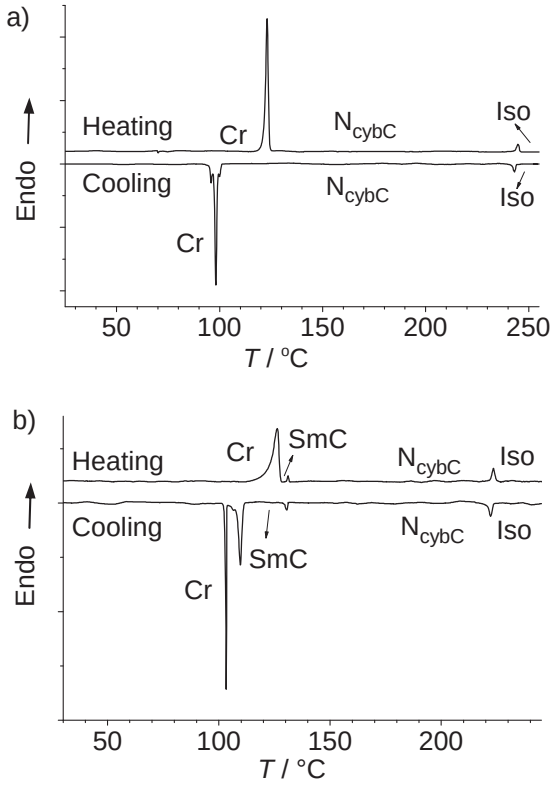

Figure 1. DSC heating and cooling traces of compounds: a) **B/5** and b) **D/5** at a rate of 10 K min^{-1}.

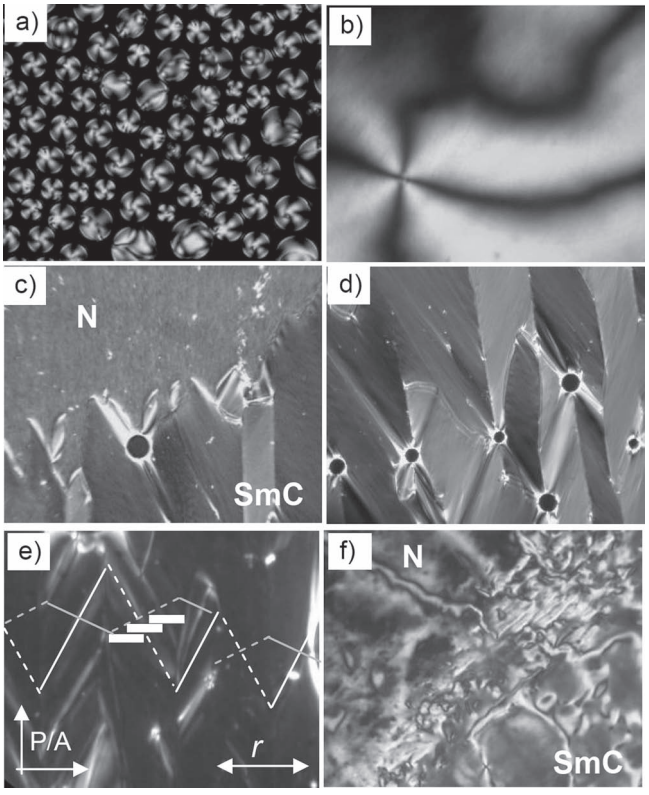

Figure 2. Microphotographs (crossed polarizers) of representative textures: a) Iso-N transition of **A/4** at $T = 293$ °C; b) N phase of the same compound at $T = 280$ °C; c) N-SmC transition as observed for compound **C/7** in a homogeneously aligned cell at $T = 173$ °C; d,e) SmC phase of the same compound at $T = 170$ °C; in e) the rubbing direction (r) is parallel to the polarizer, lines indicate the layer directions in the distinct domains with opposite tilt direction, the orientation of the rod-like cores of the molecules in one of these domains is shown as white bars; and f) N-SmC transition at $T = 173$ °C in a predominately homeotropically aligned cell. For a color version of the textures, see Figure S4 in the Supporting Information.

A/4 and **B/5** incorporating only one cyclohexane ring, reaching unusually high values of 48–50° (Table 3) which is in line with the value reported for **Ox/O9** ($\Delta\chi/2 = 49°$).[31] The $\Delta\chi/2$ splitting is considerably reduced in the nematic phases of compounds **C/7** ($\Delta\chi/2 = 20°$) and **D/5** ($\Delta\chi/2 = 36°$) incorporating two cyclohexane rings.

Table 3. XRD data of the investigated representatives of compounds A/n-D/n.[a)]

Compd.	T [°C]	L_{mol} [nm]	SAXS					WAXS	
			θ [°]	d [nm]	$\Delta\chi/2$ [°]	β_{cal} [°]	β_{opt} [°]	θ [°]	d [nm]
1,2,4-Ox/O9	150 (N)	4.9	2.05	3.07	49	51			
A/4	150 (N)	3.7	1.55	2.85	50	46		9.23	0.48
	130 (N)		1.60	2.76	50	42		9.30	0.48
B/5	150 (N)	4.0	1.39	3.19	48	37		9.16	0.48
	130 (N)		1.43	3.08	48	40		9.25	0.48
C/7	175 (N)	4.2	1.22	3.62	≈20[b)]	30		9.04	0.49
	120 (SmC)		1.28	3.44	25	35	57	9.25	0.48
D/5	150 (N)	4.2	1.17	3.77	36	26		9.06	0.49
	130 (SmC)		1.30	3.39	20	36	52	9.16	0.48

[a)]Data (θ,d) for **1,2,4-Ox/O9** were taken from ref. [31]. The molecular lengths L_{mol} were measured between the ends of the alkyl chains in a V-shaped conformation with a fixed bending angle of 140° and assuming linear all-*trans* conformation of the alkyl chains (CPK-models). β_{cal} was calculated according to $\cos\beta_{cal} = d/L_{mol}$. β_{opt} is the optical tilt determined by measuring the extinction directions of aligned samples of the SmC phases under a polarizing microscope (see Figure S5,S6 in the Supporting Information); [b)]Because magnetic aligned samples could not be obtained, and surface induced alignment did not give well aligned samples, the fitting to two maxima gave only an approximate value.

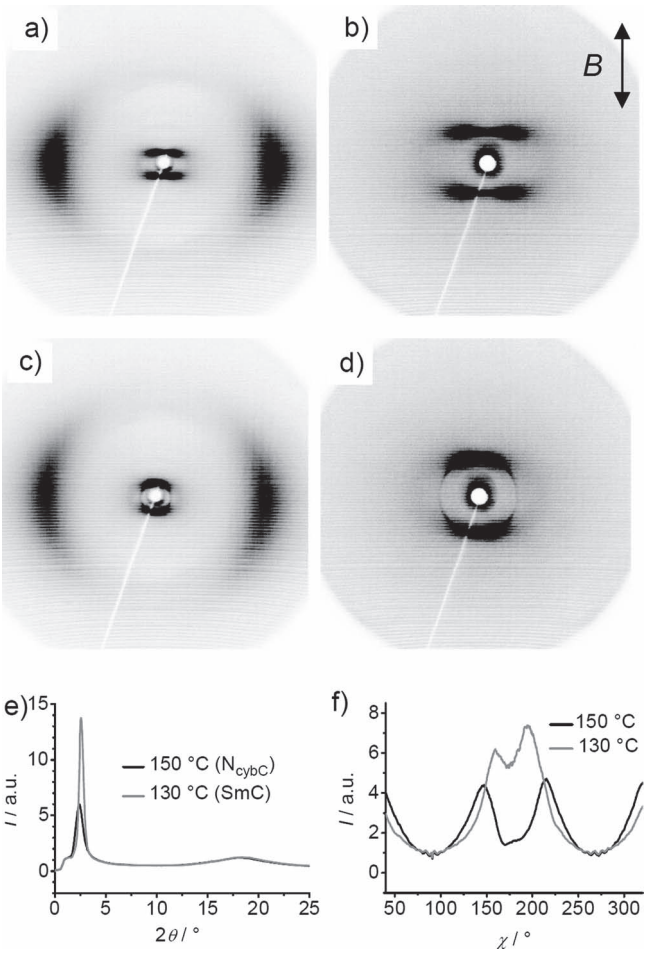

Figure 3. 2D-XRD patterns of a magnetically aligned sample of compound **D/5**. a) Complete pattern of the N phase at $T = 150$ °C and b) small-angle X-ray scattering (SAXS). c) Complete pattern of the SmC phase at $T = 130$ °C and d) SAXS (B = magnetic field direction). e) θ -scans of the diffraction patterns over the small and wide angle region. f) χ -scans over the small angle scatterings ($2\theta = 1.5$–4.5°).

Due to the limitations of our experimental setup, allowing a maximum temperature of 160 °C for the scattering experiments under a magnetic field, and the relatively high melting points of all compounds, only a limited temperature region of the nematic phase regions is accessible for investigation and therefore no clear conclusions concerning the temperature dependence of the cluster size and the tilt angle can be drawn here. However, from investigation of related compounds it is known that the cluster size is strongly temperature dependent and decreases strongly with rising temperature.[31,41] The increase of the small angle scattering intensity with decreasing temperature, as observed by comparing the diffraction patterns of the nematic phase of compound **A/4** at 130 and 150 °C (Figure S1b, Supporting Information) is in line with this general trend.

Upon cooling compound **D/5** further to $T = 131$ °C the XRD pattern changes. In the small angle region the layer reflection becomes significantly sharper, indicating the transition to a smectic phase composed of quasi infinite layers (Figure 3c–e). The wide-angle scattering remains diffuse (Figure 3e), confirming the transition to a fluid smectic phase without in-plane order. It also retains its position on the equator (Figure 3c), confirming that the alignment of the molecules remains parallel to the magnetic field direction. The splitting of the small angle reflections is significantly reduced at this transition from $\Delta\chi/2 = 36°$ in the nematic phase to only $\Delta\chi/2 = 20°$ in the SmC phase (see Figure 3d,f). However, the shift of the maximum of the small angle reflection from $d = 3.8$ nm in the nematic phase to only $d = 3.4$ nm in the smectic phase is in conflict with a reduction of the tilt at the phase transition. Indeed, optical investigation of the SmC phase of compound **D/5** indicates that the tilt of the π-conjugated aromatic cores is much stronger (optical tilt, $\beta_{opt} \approx 52°$, see Figure S6, Supporting Information) than the XRD-tilt. An even larger optical tilt of $\beta_{opt} \approx 57°$ was found for the SmC phase of compound **C/7** (Figure 2d,e and Figure S5, Supporting Information). The huge difference between XRD tilt (20–25°), providing the average tilt of the complete molecules, and optical tilt (52–57°), indicating the tilt of the π-conjugated aromatic cores, is bewildering. It seems that the major contribution to the tilt arises from the aromatic cores. In the nematic phases of compounds ***A/n*** and ***B/n*** with only one cyclohexane ring the tilt of the aromatics seems to be dominating for the observed XRD tilt. The contribution of the more disordered and hence on average less tilted aliphatic segments to the XRD-tilt is increased for compounds **C/7** and **D/5** incorporating cyclohexanes at both ends, though it seems that a strong tilt of the 3,5-diphenyl-1,2,4-oxadiazole units is retained also for these compounds. Though the optical tilt can only be measured in the SmC phases it is very likely that also in the nematic phases of compounds ***C/n*** and ***D/n*** the tilt of the aromatic cores in the SmC clusters is in the range of 40–50°. As the intensity of the two small angle reflections becomes unequal at the N-SmC phase transition the tilt in the SmC phase is synclinic (Figure 3d,f). Similar observations were made for compound **C/7** (see Table 3 and Figure S3, Supporting Information).

2.5. Electro-Optical Investigations

The four compounds **A/4**, **B/5**, **C/7** and **D/3**, representing examples for each type of compounds were also investigated by electro-optical methods. The investigations were carried out in 10 µm polyimide coated ITO cells with homogeneous alignment layers, antiparallel rubbing direction, and a measuring area of 1 cm^2.

2.5.1. Electro-Convection Patterns

For compounds **A/4**, **B/5** and **D/3** application of a DC field to the planar oriented nematic phase leads to electro-convection patterns.[43,44] **Figure 4** shows the typical change of this pattern with rising voltage for compounds **A/4** and **B/5** as examples. Also see Figure S7 and S8 in the Supporting Information.

At first, domain with equidistant stripes appear predominately parallel to the rubbing direction (Figure 4a,d). With increasing voltage the distance between the stripes decreases

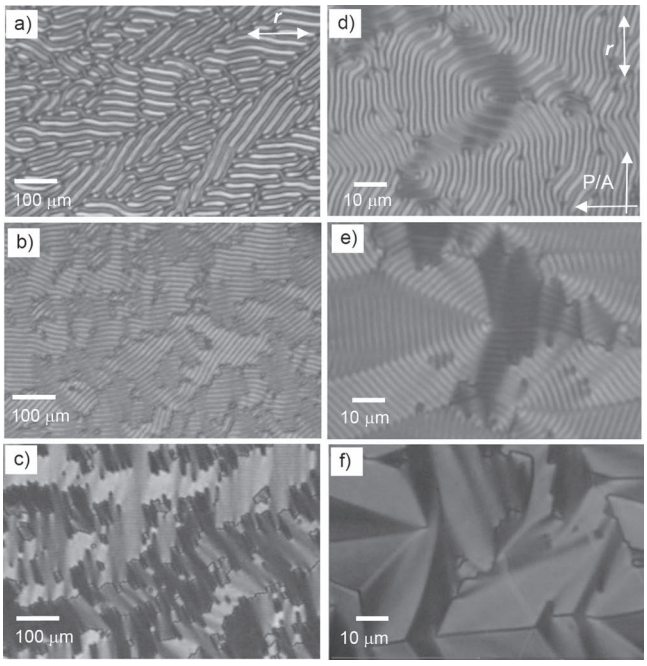

Figure 4. Field-induced texture change of the nematic phases in a 10 μm ITO PI-coated cells with planar orientation. a–c) Compound **B/5** at T = 140 °C: a) +20 V; b) +40 V; and c) +60 V. d–f) Compound **A/4** at T = 145 °C: d) +20 V; e) +40 V; and f) +60 V. For a color version of the textures see Figure S7 in the Supporting Information. See also the video in the Supporting Information.

and finally the electro-convection patterns appear similar to the texture of a smectic phase (Figure 4c,f). In this pattern the diameter of the electro-convection roles should be small and close to the wavelength of light and, hence, the periodic pattern of electro-convection walls behaves optically similar to the periodic stacking of layers in a homogeneous alignment, leading to an optical appearance with focal conic defects similar to those observed in homogeneously aligned smectic phases and short pitch cholesteric phases.[45] Similar textures have previously been reported for other nematic phases of bent-core mesogens under electric fields and their appearance was usually thought to arise from an electric field induced formation of smectic phases.[34] However, it seems that in most cases these textures are due to electro-convection. This is supported by the fact that for compound **C/7** with a SmC-N-dimorphism no electro-convection pattern and also no field-induced fan-shaped texture can be observed (see **Figure 7**b–d) in the whole temperature range of the nematic phase, even close to the N-to-SmC transition. In contrast, for compounds **A/4** and **B/5** without any smectic low temperature phase, but showing electro-convection patterns, the fan-shaped texture can be observed above a certain voltage in the whole temperature range of the N phase. A video showing one switching cycle of **A/4** under a 0.02 Hz triangular wave field is included in the Supporting Information.

No textures were discussed for the previously reported compound **1,2,4-Ox/O9**, but the absence of a field induced smectic phase was confirmed for the nematic phase of this compound by synchrotron XRD experiments in ITO-coated cells, where the diffuse four spot pattern turns into a diffuse ring under an applied electric field above a certain threshold voltage (**Figure 5**b).[31] This confirms that no layer structure is induced (diffraction remains diffuse) and that uniform alignment in the cell is lost (change from four-spot pattern to diffuse ring), most probably, due to electro-convection. After the field was switched off the four spot pattern was restored (Figure 5a) after ≈2 s, which exceeds the time required for the complete relaxation of the electro-convection pattern to a homogeneously aligned texture at 0 V.

2.5.2. Electro-Optical Investigations Under Triangular Wave Fields

Upon application of a triangular wave voltage of frequency 10 Hz for all four compounds a single peak per half cycle of the applied voltage was observed in the current curves (**Figure 6**a and Supporting Information Figure S9). It could be argued that the formation of electro-convection patterns requires the transport of charges and this ion-conduction could be a possible origin of the peak in the current curves. However, electro-convection patterns were observed in the nematic phases of most other bent-core mesogens[44] for which no current peak was observed,[41] and in the case of the 1,2,4-oxadiazoles, the current peak was observed even if no electro-convection was found, as for example in the case of compound **C/7** (see **Figure 7**a–d). For this compound the shape of the current curves in the nematic phase are very similar to those of the other compounds and the current response is even the highest of all investigated compounds (measured in 10 μm cell).

For all investigated compounds the current response peak occurs above a certain threshold voltage. The threshold voltage is about 8 V_{pp} μm^{-1} for compounds **A/4**, **B/5**, and **C/7**, whereas for compound D/**3** it is 16 V_{pp} μm^{-1}. Figure 6a,b shows the current response curve at T = 140 °C (V_{pp} = 80 V) and the dependence of the peak area on temperature for compound **B/5** as an example; for the other investigated compounds these diagrams are shown in Figure S9 (Supporting Information).

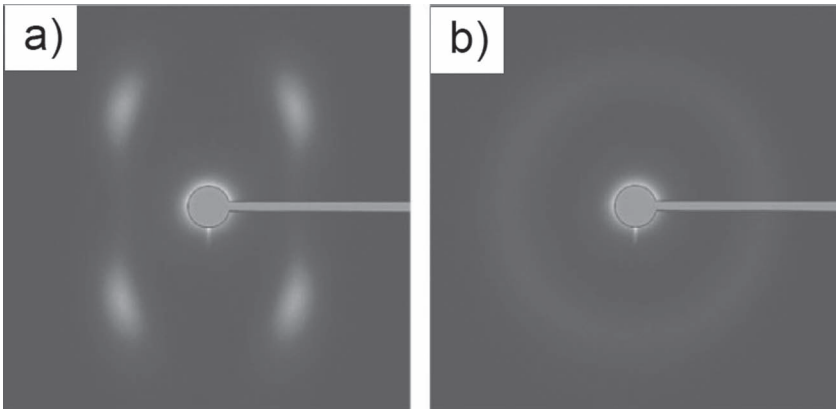

Figure 5. Synchrotron XRD patterns from a 20 μm sample of compound **1,2,4-Ox/O9** subjected to a square-wave voltage: a) before and b) after the voltage step rise corresponding to the onset of the switching repolarization current peak. Reproduced with permission.[31]

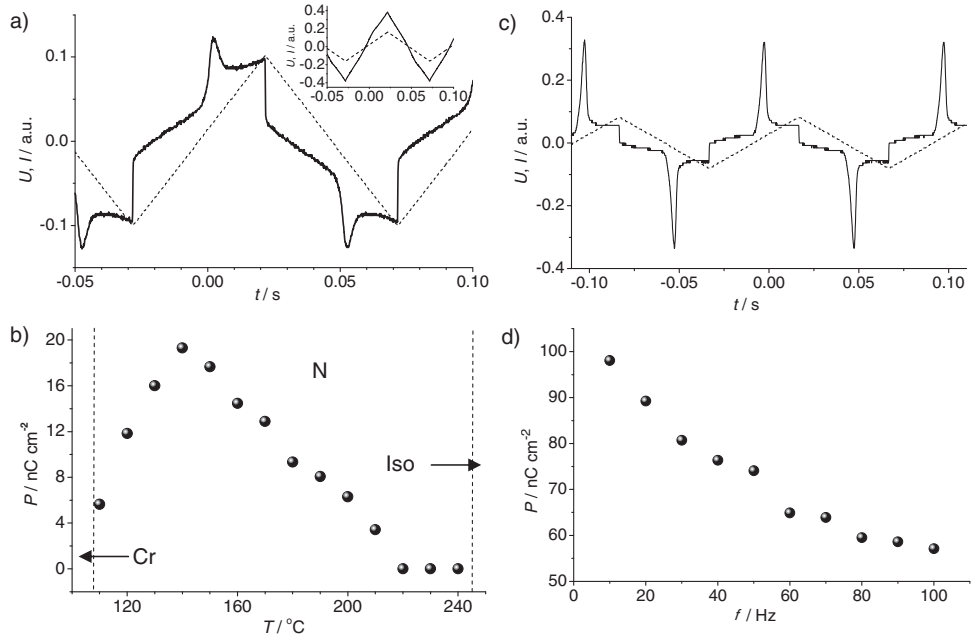

Figure 6. Investigation of compound **B/5**: a) current response at 140 °C in a 10 µm ITO-coated cell with homogeneous alignment under a triangular wave field with 80 V_{pp}, 10 Hz, and 5 kΩ. The dotted line indicates the applied triangular wave voltage. The inset shows the absence of a current response in the isotropic phase at T = 250 °C. b) Peak area (plotted as polarization P) as function of temperature (V_{pp} = peak-to-peak voltage) as measured at T = 140 °C in a 10 µm ITO cell. c) Current response at T = 140 °C in a 2 µm ITO-coated cell with homogeneous alignment under triangular wave field with 80 V_{pp} 5 kΩ. In (a,c) the doted lines indicates the applied triangular wave voltage, the solid lines the current response. d) Polarization (P in nC cm^{-2}) as a function of frequency (ν in Hz) as measured at T = 140 °C in a 2 µm ITO cell at 80 V_{pp}.

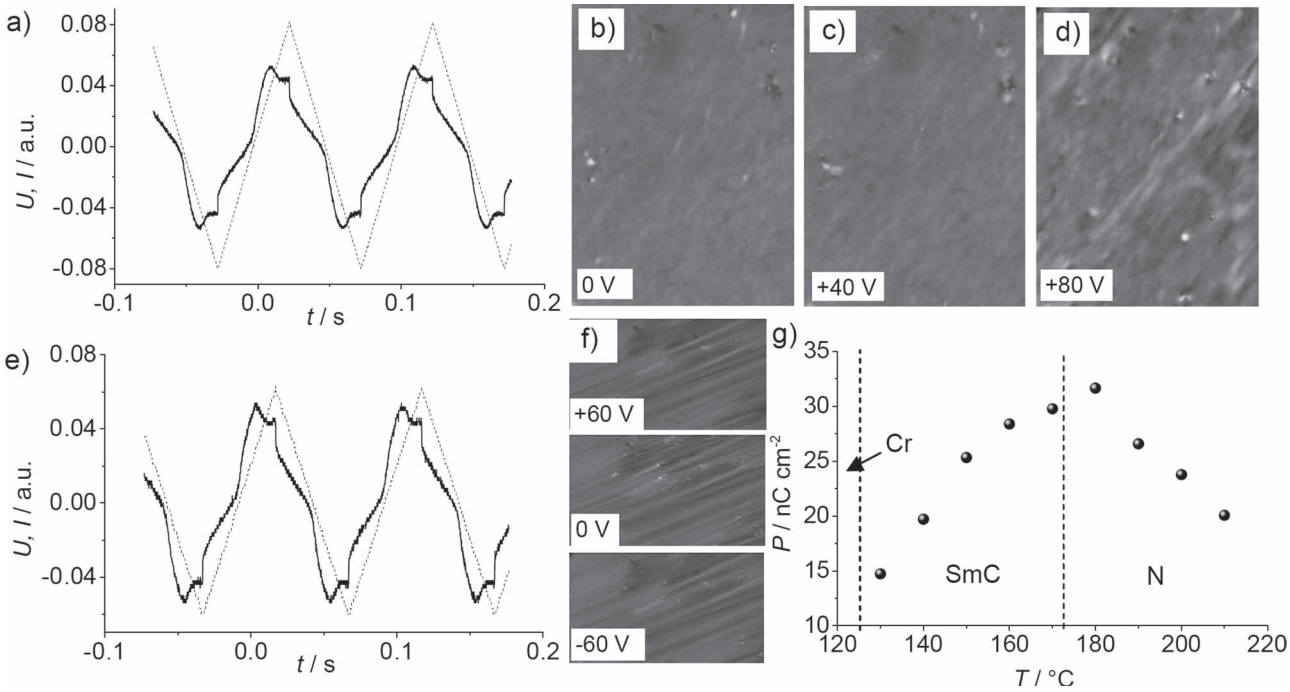

Figure 7. Electro-optic investigations of compound **C/7** in a 10 µm PI-coated ITO cell with homogeneous alignment layer. a) Current response (red line) in the N phase at T = 180 °C, 80 V_{pp}, 10 Hz, 5 kΩ. The dotted line indicates the triangular wave voltage. b–d) Textures in the nematic phase at T = 200 °C under a DC voltage of b) 0 V, c) +40 V, and d) +80 V showing the absence of electro-convection patterns. e) Current response in the SmC phase at T = 160 °C, 80 V_{pp}, 10 Hz, 5 kΩ. f) Textures of the SmC phase at T = 150 °C under DC voltages of +60 V, 0 V, and –60 V showing that the texture is not changed by reversing the applied field and g) polarization at 80 V_{pp}, 10 Hz, as a function of temperature (crystallization takes place below 130 °C, above 210 °C decomposition sets in). For a color version of the textures see Figure S12 in the Supporting Information.

The peak area only marginally increases upon further increase of the applied voltage after the threshold voltage is reached, however, it is strongly temperature dependent (Figure 6b). The maximum values of peak area were observed at a distinct temperature which is in a temperature range between 140 and 180 °C and decreases gradually towards higher and lower temperatures. In the isotropic phase the peak has completely disappeared in all cases. Both, the shape of current response curve as well as the temperature dependence are nearly identical for all compounds and are also similar to that reported for **1,2,4-Ox/O9**.[31] The fact that already before approaching the transition to the isotropic phase the current peak completely disappeared (inset of Figure 6a), seems to rule out the possibility that it is due to ionic conduction. The peak is also observed in non-coated ITO cells (see Figure S10 in the Supporting Information), hence formation of an electric double layer can also not explain the current peak. Assuming a polarization (P) as the origin of this current peak, polarization values between $P = 12$ and 32 nC cm^{-2} could be calculated for the maximum current values observed for these compounds (see also Figure S9b,d in the Supporting Information) in 10 µm cells. As shown for compound **B/5** the current response rises to values corresponding to $P = 100$ nC cm^{-2} in a 6 µm cell (Figure S11a, Supporting Information) and remains nearly constant upon further reduction of the cell gap to 2 µm (Figure 6c). This observation does not agree with a conductivity effect, which would be expected to lead to a continuous increase of the current upon reduction of the sample thickness. Instead, this non-linear dependence on cell thickness with a distinct saturation value is similar to the behavior of SmC* phases where the field induced polarization was found to increase with growing cell thickness and stabilizes at a certain thickness.[46] The plot of P as a function of frequency in Figure 6d clearly shows a gradual decrease with rising frequency. This dependence is in the same way as the dependence of polarization versus frequency of the slowest relaxation process (see Section 2.6).

For compound **C/7** with a N-SmC transition the polarization peak starts decreasing around the N-to-SmC transition (Figure 7g) as it was also observed for compound **1,2,4-Ox/O9**.[31] The relatively broad shape of the current peak in the N and SmC phase is similar to that found in SmAP$_R$ phases.[47–49] The common characteristics of SmAP$_R$ phases is that in the ground state the polar direction of short range correlated molecular dipoles is randomized leading to a macroscopic uniaxial and nonpolar smectic phase. Application of an electric field cooperatively orients the dipoles and increases the correlation length of polar order in the layers and a switching of the field induced polar domains with finite correlation length can be observed under a sufficiently strong external field. It takes place between the applied field and the dipoles and against thermal agitation (Langevin process).[47a] It appears possible that a similar process could take place in the nematic phases of all 1,2,4-oxadiazole compounds and also in the SmC phases of compound **C/7** and **D/5**.

In the nematic and SmC phases of the investigated compounds no change of the texture could be observed by field reversal (see Figure 7f). As XRD investigations indicate that the tilt is synclinic in the SmC phase, this could be explained with a switching process taking place by rotation around the molecular long axis.[50] As in this process the orientation of the director is not changed the texture would be retained though the polar direction is reversed.

2.6. Dielectric Spectroscopy

Compound **B/5** was investigated by dielectric spectroscopy with a weak applied field (0.1 V µm^{-1}) in the frequency range between 5 Hz to 10 MHz and at temperatures between 107 and 227 °C. The temperature-dependent complex dielectric permittivity was measured for both planar and homeotropic anchoring conditions. Homeotropic alignment was obtained by applying a magnetic field of $B = 1.2$ T to the cell and the dielectric measurements were made with the magnetic field applied to the cell. For a better resolution of the peaks, the derivative of the real part of permittivity, $d\varepsilon'/d(\ln f)$[51] (see **Figure 8**) has been analyzed. Figure 8a,b show the frequency dependence of the derivative of the parallel component of ε', i.e., $d\varepsilon'_{\parallel}/d(\ln f)$ (measured for homeotropic anchoring) and the derivative of perpendicular component of ε', $d\varepsilon'_{\perp}/d(\ln f)$ (measured for planar anchoring), respectively, for different temperatures in the nematic phase.

The plot at 157 °C in the nematic phase (Figure 8c) shows three relaxation peaks in the measured frequency range for both planar and homeotropic conditions. The peaks P2 and P3 are attributed to molecular processes. P2 is due to the rotation around the short axis and P3 is assigned to the rotation around the long molecular axis. The temperature dependence of the dielectric strengths ($\delta\varepsilon_2$ and $\delta\varepsilon_3$) and the relaxation frequencies (f_2 and f_3) of these modes are given in Figure S15 (Supporting Information). The dielectric strength of P2 shows $(1 + 2S)$ dependence on temperature, where S is the orientational order parameter of the long axis, whereas that of P3 shows $(1 - S)$ dependence on temperature. This is in accordance with the theory of Coffey and Kalmykov.[52] These authors have extended the theory of Maier and Saupe for the generalized case of the dipole moment lying at an angle to the symmetry axis of the molecule that was assumed to be ellipsoidal. They derived analytical expressions for the frequency-dependent complex permittivity in terms of the relaxation times of the relevant processes, the molecular parameters and the orientational order parameter. The observed dielectric strengths correspond to those calculated theoretically. The peak P2, is expected to appear only in $d\varepsilon'_{\parallel}d(\ln f)$. However its presence in $d\varepsilon'_{\perp}/d(\ln f)$ (whereas it is four times weaker) is mainly due to the reason that the smectic orientational order parameter S of the system is less than unity as well as there is a significant pre-tilt of the director to the substrate.

The lowest frequency process P1 is attributed to the collective motion of the molecules due to the following reasons. First, the temperature dependence of the dielectric strength ($\delta\varepsilon_1$) and the relaxation frequency (f_1) of the process P1 shows very large values of $\delta\varepsilon$, of the order of 230 (Figure 8d). The second reason is that the observed polarization (Figure 6d) depends on frequency. The polarization is observed to decrease with increase in frequency higher than a few tens of Hz as full switching is not possible within the half period of the applied voltage. The third reason is that for a particular temperature the frequency at which the polarization value decreases (at 140 °C, it is ≈100 Hz) corresponds to the relaxation frequency of P1 at that temperature (Figure 8d and 6d).

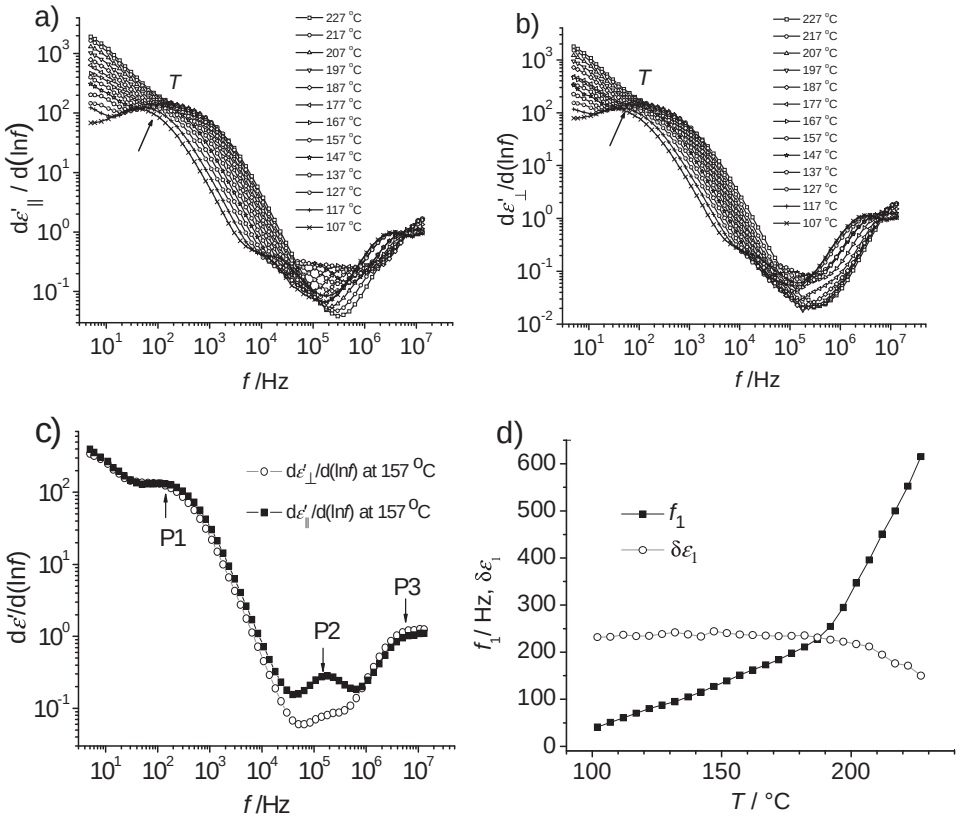

Figure 8. Dielectric spectroscopy of compound **B/5**: a,b) Frequency dependence of d $\varepsilon'_{\parallel}$/d(ln f) and d $\varepsilon'_{\perp}$/d(ln f) for different temperatures; c) d ε'/d(ln f) vs. frequency plot at 157 °C (nematic phase) for planar (○) and homeotropic (■) orientations. P1, P2 and P3 are different relaxation processes; and d) temperature dependence of relaxation frequency (■) and the dielectric strength (○) of the process P1. For a color version of the graphs in (a,b) see Figure S14 in the Supporting Information.

The size of the polar domains was estimated from the strength of the P1 peak ($\delta\varepsilon = 230$), assuming the lateral dipole moment of the molecules to be 5 D[31] and T = 140 °C to be in the range of about 90 molecules aligned parallel. This corresponds quite well to the cluster size determined for the ground state of the N_{cybC} phase of this compound by XRD (about 6 × 6 molecules and two layers, see Section 2.4). This also corresponds well with previously reported simulation results predicting a polar order in the cybotactic clusters.[31]

3. Summary and Conclusions

In summary, new types of 1,2,4-oxadiazole based bent-core LC incorporating cyclohexane unit(s) have been synthesized, among them first examples of unsymmetrically substituted 1,2,4-oxadiazoles. These molecules form cybotactic nematic phases composed of SmC-like clusters (N_{cybC} phases) over broad temperature ranges, in two cases accompanied by a nematic-to-SmC transition at lower temperature. In all LC phases the aromatic cores have an unusual high tilt between 40 and 57°. In their nematic phase regions all compound show a single and relatively broad current peak under an applied triangular wave voltage above a certain threshold voltage with the same characteristics as previously reported for compound **1,2,4-Ox/O9**.[31] Hence, this current peak seems to be a rather general feature of bent-core mesogens based on the 3,5-diphenyl-1,2,4-oxadiazole bent core unit. It also seems to be specific for the nematic phases of 1,2,4-oxadiazole based bent core mesogens as such a peak was not observed in the N_{cybC} phases of other investigated bent-core LCs, like the isomeric 1,3,4-oxadiazole **1,3,4-Ox/O8** (see Scheme 1, $n = 8$)[53] and the series of 4–cyanoresorcinols.[41] Even under applied fields up to 20 V_{pp} μm^{-1} no current peak could be detected in the whole nematic phase range of these compounds (see Figure S13, Supporting Information).[54]

Electro-optical and dielectric investigations are in line with a ferroelectric-like polar switching and not with a DC conductivity as origin of this peak. The presence of a considerable threshold voltage excludes a true ferroelectric switching process with two stable polar ground states. It appears more likely that polar order in the nematic phase is induced under the applied electric field in a similar way as previously found for $SmAP_R$ phases (Langevin process).[47] Additionally, the shape and position of the peak is similar to $SmAP_R$ phases. However, for the compounds under discussion the field induced formation of a smectic phase can be excluded based on our electro-optical investigations and previous XRD studies.[31] Moreover, the dielectric results (Section 2.6) indicate that already at low field strength (0.1 V μm^{-1}) the correlation length of the polar order corresponds to the size of the cybotactic clusters. The

weak effect of the AC and DC voltage amplitude on the dielectric strength also suggests that even in the ground state the dipole correlation length comparable to the cluster size. Hence, there is appreciable local polar order in the randomly organized cybotactic clusters (SmCP-like clusters) and the phases are assigned as N_{cybCP} phases. The observation that the collective fluctuations are not quenched by a bias field (biasing with 1 V μm^{-1} decreases the dielectric strength by less than 10%) is in contrast to $SmAP_R$ phases where the dielectric strength strongly decreases with increasing bias field because in the layers the reorientations of the dipoles are suppressed by the bias.[47] However, in the N_{cybCP} phases the correlation length of the dipoles is limited by the cluster size, and therefore, the polar correlation length becomes nearly independent on the bias field. Though there is local polar order, the polar directions are randomized in the apolar ground state. There is a relatively high threshold for ferroelectric-like switching (8 V μm^{-1}) that seems to be required for removing the modulation of polar order, i.e., to align the polar cybotactic clusters of the N_{cybCP} phase. In these N_{cybCP} phases the formation of a non-modulated polar structure is not supported by the presence of quasi infinite interlayer interfaces, as it is the case in the $SmAP_R$ phases. Therefore, the applied electric field must work against thermal agitation and the antipolar packing of the cybotactic clusters in order to align them with uniform polar direction in a Langevin process of polar ordering ($\mu_{eff}E/kT \approx 1$ at $E = 6$ V μm^{-1} for the cluster size estimated is in the range of the threshold of 8 V μm^{-1} required for polar switching).

Overall, these investigations strongly corroborate the model proposed previously,[31] i.e., the uniaxial nematic phases of these compounds are formed by polar cybotactic clusters and the major effect of the electric field is to align these polar clusters.[31] Polar order in the clusters leads to local biaxiality, which becomes macroscopic in the field induced polar states. As the molecules are tilted, the field induced polar biaxial nematic state N_b^P has C_2 symmetry and can be considered as the polar variant of the monoclinic biaxial nematic phase (N_{bm}).[21,26]

It is likely that in the ferroelectric-like switching process the direction of the induced polarization is reversed through cooperative rotation of the molecules around their long axis[50] as known for other bent-core mesogens with a relatively weak bend and in line with electro-optic investigation of the SmC phase of **C/7** (Figure 7f). Due to the chiral C_2 symmetry of the field induced polar state the reversal of the field direction by rotation around the long axis should result in a reversal of chirality,[50] which is an interesting point for further investigations.

In the SmC phase the relatively low polarization value and the broad shape of the peak suggest that also in this phase the polarization is only short range and macroscopic polarization is induced under an applied electric field. In this respect the SmC phase can be regarded as a LC phase with a randomized local polarization, similar to the non-tilted $SmAP_R$ phases (SmC_R phases). The reduction of P with decreasing temperature is also observed for $SmAP_R$ phases[47,48] and is most probably due to the increasing viscosity.[55] Thus, it seems that randomized polar phases ($SmAP_R$, $SmCP_R$, N_{cybCP}, etc.), unknown for rod-like LCs as well as for typical bent-core mesogens, with a solid bending angle around 120° can be regarded as a new class of LC phases occurring at the transition from a rod-like to a bent molecular shape.

As a second important result of these studies it was found that under high fields electro-convection patterns in the nematic phases of bent-core molecules can appear with textures very similar to the fan-textures of homogeneously aligned smectic and cholesteric phases. These patterns can be formed under AC as well as DC fields and hence care is required by interpreting these field induced textures as field induces smectic phases.

Supporting Information

Supporting Information is available from the Wiley Online Library or from the author. It includes synthetic procedures, analytical data, additional XRD data, PM pictures, data of electro-optic and dielectric studies, and color versions of the textures in Figure 2, 4, and 7 as well as the multiplot diagrams Figure 8a,b. A video showing the switching of compound **A/4** in the nematic phase under an triangular electric wave field of $f = 0.02$ Hz, 120 V_{pp} in a 10 µm polyimide-coated ITO cell at $T = 145$ °C between crossed polarizers is also included.

Acknowledgements

This work was supported by the EU within the FP7 funded Collaborative Project BIND (Grant No 216025). The authors thank J. P. F. Lagerwall, Seoul National University, for fruitful discussions.

Received: July 31, 2011
Revised: November 24, 2011
Published online: February 7, 2012

[1] a) H. Ringsdorf, B. Schlarb, J. Venzmer, *Angew. Chem. Int. Ed. Engl.* **1988**, *27*, 113; b) G. M. Whitesides, B. Grzybowski, *Science* **2002**, *295*, 2418; c) T. Kato, *Science* **2002**, *295*, 2414; d) J. W. Goodby, I. M. Saez, S. J. Cowling, V. Görtz, M. Draper, A. W. Hall, S. Sia, G. Cosquer, S. E. Lee, E. P. Raynes, *Angew. Chem. Int. Ed.* **2008**, *47*, 2754; e) C. Tschierske, *Chem. Soc. Rev.* **2007**, *36*, 1930.

[2] C. Hilsum, *Philos. Trans. R. Soc. A.* **2010**, *368*, 1027.

[3] a) B. R. Kaafarani, *Chem. Mater.* **2011**, *23*, 378; b) L. Vicari, *Optical Applications of Liquid Crystals*, Institute of Physics Publishing, Bristol and Philadelphia **2003**.

[4] H. Yang, G. Ye, X. Wang, P. Keller, *Soft Matter* **2011**, *7*, 815.

[5] Y. H. Kim, D. Ki. Yoon, H. Su. Jeong, O. D. Lavrentovich, H.-T. Jung, *Adv. Funct. Mater.* **2011**, *21*, 610.

[6] W.-J. Chung, A. Merzlyak, S.-W. Lee, *Soft Matter* **2010**, *6*, 4454.

[7] a) S. Sivakumar, K. L. Wark, J. K. Gupta, N. L. Abbott, F. Caruso, *Adv. Funct. Mater.* **2009**, *19*, 2260; b) A. Agarwal, E. Huang, S. Palecek, N. L. Abbott, *Adv. Mater.* **2008**, *20*, 4804; c) A. Angelova, B. Angelov, R. Mutafchieva, S. Lesieur, P. Couvreur, *Acc. Chem. Res.* **2011**, *44*, 147; d) H. Tan, S. Yang, G. Shen, R. Yu, Z. Wu, *Angew. Chem. Int. Ed.* **2010**, *49*, 8608; e) A. D. Rey, *Soft Matter* **2010**, *6*, 3402.

[8] a) G. T. Stewart, *Liq. Cryst.* **2004**, *31*, 443; b) J. Lydon, *Liq. Cryst. Today* **2006**, *15*, 1; c) M. Nakata, G. Zanchetta, B. D. Chapman, C. D. Jones, J. O. Cross, R. Pindak, T. Bellini, N. A. Clark, *Science.* **2007**, *318*, 1276.

[9] a) P. J. Collings, M. Hird, *Introduction to Liquid Crystals*, Taylor & Francis, London **1997**; b) D. Demus, J. W. Goodby, G. W. Gray, H.-W, Spiess, V. Vill, *Handbook of Liquid Crystals*, *Vol.*1-3, Wiley-VCH, Weinheim **1998**.
[10] a) T. Sekine, T. Niori, J. Watanabe, T. Furukawa, S. W. Choi, H. Takezoe, *J. Mater. Chem.* **1997**, *8*, 1307; b) L. E. Hough, M. Spannuth, M. Nakata, D. A. Coleman, C. D. Jones, G. Dantlgraber, C. Tschierske, J. Watanabe, E. Körblova, D. M. Walba, J. E. Maclennan, M. A. Glaser, N. A. Clark, *Science* **2009**, *325*, 452; c) C. Tschierske, in *Chirality at the nano scale*, (Ed: D. B. Amabillino), Wiley-VCH, Weinheim **2009**, 271.
[11] T. Niori, T. Sekine, J. Watanabe, T. Furukawa, H. Takezoe, *J. Mater. Chem.* **1996**, *6*, 1231.
[12] D. R. Link, G. Natale, R. Shao, J. E. Maclennan, N. A. Clark, E. Körblova, D. M. Walba, *Science* **1997**, *278*, 1924.
[13] a) R. A. Reddy, C. Tschierske, *J. Mater. Chem.* **2006**, *16*, 907; b) H. Takezoe, Y. Takanishi, *Jpn. J. Appl. Phys.* **2006**, *45*, 597; c) J. Etxebarria, M. Blanca, *J. Mater. Chem.* **2008**, *18*, 2919.
[14] D. Girdiziunaite, C. Tschierske, E. Novotna, H. Kresse, *Liq. Cryst.* **1991**, *10*, 397. L. A. Karamysheva, S. I. Torgova, I. F. Agafonova, V. F. Petrov, *Liq. Cryst.* **2000**, *27*, 393.
[15] a) L. A. Madsen, T. J. Dingemans, M. Nakata, E. T. Samulski, *Phys. Rev. Lett.* **2004**, *92*, 145505; b) B. R. Acharya, A. Primak, S. Kumar, *Phys. Rev. Lett.* **2004**, *92*, 145506; c) B. R. Acharya, A. Primak, T. J. Dingemans, E. T. Samulski, S. Kumar, *Pramana* **2003**, *61*, 231; d) L A. Madsen, T. J. Dingemans, M. Nakata, E. T. Samulski, *Phys. Rev. Lett.* **2006**, *96*, 219804; e) K. J. Semmler, T. J. Dingemans, E. T. Samulski, *Liq. Cryst.* **1998**, *24*, 799; f) T. J. Dingemans, E. T. Samulski, *Liq. Cryst.* **2000**, *27*, 131; g) T. J. Dingemanns, L. A. Madsen, N. A. Zafiropoulos, W. Lin, E. T. Samulski, *Philos. Trans. R. Soc. A* **2006**, *364*, 2681; h) N. A. Zafiropoulos, W. Lin, E. T. Samulski, T. J. Dingemans, S. J. Picken, *Liq. Cryst.* **2009**, *36*, 649.
[16] a) J.-H. Lee, T.-K. Lim, W.-T. Kim, J. I. Jin, *J. Appl. Phys.* **2007**, *101*, 034105; b) R. Stannarius, *J. Appl. Phys.* **2008**, *104*, 036104.
[17] a) M. Lehmann, C. Köhn, H. Kresse, Z. Vakhovskaya, *Chem. Commun.* **2008**, 1768; b) P. J. Martin, D. W. Bruce, *Liq. Cryst.* **2007**, *34*, 767; c) S.-W. Choi, S. Kang, Y. Takanishi, K. Ishikawa, J. Watanabe, H. Takezoe, *Chirality* **2007**, *19*, 250; d) D. Apreutesei, G. H. Mehl, *J. Mater. Chem.* **2007**, *17*, 4711.
[18] a) V. Görtz, J. W. Goodby, *Chem. Commun.* **2005**, 3262; b) C. D. Southern, P. D. Brimicombe, S. D. Siemianowski, S. Jaradat, N. Roberts, V. Görtz, J. W. Goodby, H. F. Gleeson, *Eur. Phys. Lett.* **2008**, *82*, 56001; c) Y. Xiang, J. W. Goodby, V. Görtz, H. F. Gleeson, *Appl. Phys. Lett.* **2009**, *94*, 193507; d) V. Görtz, C. Southern, N. W. Roberts, H. F. Gleeson, J. W. Goodby, *Soft Matter* **2009**, *5*, 463.
[19] G. Pelzl, W. Weissflog, in *Thermotropic Liquid Crystals: Recent Advances* (Ed: A. Ramamoorthy), Springer, Berlin **2007**, *Ch. 1*, pp. 1–58.
[20] M. J. Freiser, *Phys. Rev. Lett.* **1970**, *24*, 1041.
[21] C. Tschierske, D. J. Photinos, *J. Mater. Chem.* **2010**, *20*, 4283.
[22] a) G. R. Luckhurst, *Thin Solid Films* **2001**, *393*, 40; b) K. Praefcke, *Mol. Cryst. Liq. Cryst.* **2001**, *364*, 15; c) G. R. Luckhurst, *Angew. Chem. Int. Ed.* **2005**, *44*, 2834; d) D. W. Bruce, *Chem. Rec.* **2004**, *4*, 10; e) Y. Galerne, *Phys. Rev. Lett.* **2006**, **96**, 219803.
[23] K. V. Le, M. Mathews, M. Chambers, J. Harden, Q. Li, H. Takezoe, A. Jakli, *Phys. Rev. E: Stat., Nonlinear, Soft Matter Phys.* **2009**, *79*, 030701.
[24] R. Berardi, L. Cuccioli, C. Zannoni, *J. Chem Phys.* **2008**, *128*, 024905.
[25] a) R. Berardi, C. Zannoni, *J. Chem. Phys.* **2000**, **113**, 5971; b) T. C. Lubensky, L. Radzihovsky, *Phys. Rev. E* **2002**, **66**, 031704; c) J. Pelaez, M. R. Wilson, *Phys. Rev. Lett.* **2006**, *97*, 267801.
[26] a) A. G. Vanakaras, D. J. Photinos, *J. Chem. Phys.* **2008**, *128*, 154512; b) S. D. Peroukidis, P. K. Karahaliou, A. G. Vanakaras, D. J. Photinos, *Liq. Cryst.* **2009**, *36*, 727; c) P. K. Karahaliou, A. G. Vanakaras, D. J. Photinos, *J. Chem. Phys.* **2009**, *131*, 124516; d) S. Droulias, A. G. Vanakaras, D. J. Photinos, *Liq. Cryst.* **2010**, *37*, 969.
[27] a) O. Francescangeli, F. Vita, C. Ferrero, T. Dingemans, E. T. Samulski, *Soft Matter* **2011**, *7*, 895; b) O. Francescangeli, E. T. Samulski, *Soft Matter* **2010**, *6*, 2413.
[28] a) H. Gallerdo, I. M. Begini, *Mol. Cryst. Liq. Cryst.* **1995**, *258*, 85; b) M. L. Parra, P. I. Hidalgo, E. Y. Elgueta, *Liq. Cryst.* **2008**, *35*, 823; c) H. Gallardo, R. Cristiano, A. A. Vieira, F. Neves, A. W. Ricardo, R. M. Srivastava, *Synthesis* **2008**, 605; d) H. Gallardo, R. Cristiano, A. A. Vieira, F. Neves, A. W. Ricardo, R. M. Srivastava, I. H. Bechtold, *Liq. Cryst.* **2008**, *35*, 857; e) M. L. Parra, P. I. Hidalgo, E. A. Soto-Bustamante, J. Barbera, E. Y. Elgueta, V. H. Rrujillo-Rojo, *Liq. Cryst.* **2008**, *35*, 1251.
[29] a) S. I. Torgova, T. A. Geivandova, O. Francescangeli, A. Strigazzi, *Pramana* **2003**, *61*, 239; b) L. A. Karamysheva, I. F. Agafonova, T. A. Geivandova, S. I. Torgova, M. Becchi, *SPIE* **2002**, *4759*, 49; c) S. I. Torgova, L. A. Karamysheva, T. A. Geivandova, A. Strigazzi, *Mol. Cryst. Liq. Cryst.* **2001**, *365*, 99.
[30] Previously reported cyclohexane-substituted 1,2,4-oxadiazoles incorporated the cyclohexane ring directly attached to the aromatic core via a single bond [4(4-alkylcyclohex-1-yl)benzenes]: a) L. A. Karamysheva, I. F. Agafonova, S. I. Torgova, *Mol. Cryst. Liq. Cryst.* **1999**, *332*, 407; b) L. A. Karamysheva, S. I. Torgova, I. F. Agafonova, N. M. Shtykov, *Mol. Cryst. Liq. Cryst.* **1995**, *360*, 217; c) L. A. Karamysheva, I. F. Agafonova, S. I. Torgova, V. I. Torgov, *Mol. Cryst. Liq. Cryst.* **2000**, *352*, 327. d) S. I. Torgova, L. A. Karamysheva, A. Strigazzi, *Braz. J. Phys.* **2002**, *32*, 593.
[31] O. Francescangeli, V. Stanic, S. I. Torgova, A. Strigazzi, N. Scaramuzza, C. Ferrero, I. P. Dolbnya, T. M. Weiss, R. Berardi, L. Muccioli, S. Orlandi, C. Zannoni, *Adv. Funct. Mater.* **2009**, *19*, 2592.
[32] H. Takezoe, J. Watanabe, *Mol. Cryst. Liq. Cryst.* **1999**, *328*, 325.
[33] A. Lesac, H. L. Nguyen, S. Narancic, U. Baumeister, S. Diele, D. W. Bruce, *Liq. Cryst.* **2006**, *33*, 167.
[34] a) G. Pelzl, A. Eremin, S. Diele, H. Kresse, W. Weissflog, *J. Mater. Chem.* **2002**, *12*, 2591; b) W. Weissflog, S. Sokolowski, H. Dehne, B. Das, S. Grande, M. W. Schröder, A. Eremin, S. Diele, G. Pelzl, H. Kresse, *Liq. Cryst.* **2004**, *31*, 923; c) L. Kovalenko, M. W. Schröder, R. A. Reddy, S. Diele, G. Pelzl, W. Weissflog, *Liq. Cryst.* **2005**, *32*, 857; d) M. G. Tamba, B. Kosata, K. Pelz, S. Diele, G. Pelzl, Z. Vakhovskaya, H. Kresse, W. Weissflog, *Soft Matter* **2006**, *2*, 60.
[35] G. Shanker, C. Tschierske, *Tetrahedron* **2011**, *67*, 8635.
[36] a) B. Neises, W. Steglich, *Angew. Chem. Int. Ed. Engl.* **1978**, *17*, 522; b) J. C. Sheehan, J. J. Hlavka, *J. Org. Chem.* **1956**, *21*, 439; c) C. Tschierske, H. Zaschke, *J. Prakt. Chem.* **1989**, *331*, 365–366.
[37] a) S. Stojadinovic, A. Adorjan, S. Sprunt, H. Sawade, A. Jakli, *Phys. Rev. E* **2002**, *66*, 060701; b) D. Wiant, S. Stojadinovic, K. Neupane, S. Sharma, K. Fodor-Csorba, A. Jakli, J. T. Gleeson, S. Sprunt, *Phys. Rev. E* **2006**, *73*, 030703; c) N. Vaupotic J. Szydlowska, M. Salamonczyk, A. Kovarova, J. Svoboda, M. Osipov, D. Pociecha, E. Gorecka, *Phys. Rev. E* **2009**, *80*, 030701.
[38] A. Guinier, *X-ray Diffraction*, Freeman, San Francisco **1963**.
[39] O. Francescangeli, M. Laus, G. Galli, *Phys. Rev. E* **1997**, *55*, 481.
[40] a) A. de Vries, *Pramana, Suppl.* **1975**, *1*, 93; b) A. de Vries, *J. Mol. Liq.* **1986**, *31*, 193; c) P. Sarkar, P. K. Sarkar, S. Paul, P. Mandal, *Phase Transitions* **2000**, *71*, 1.
[41] C. Keith, A. Lehmann, U. Baumeister, M. Prehm, C. Tschierske, *Soft Matter* **2010**, *6*, 1704.
[42] H. Takezoe, Y. Takanishi, *Jpn. J. Appl. Phys. Part 1.* **2006**, *45*, 597.
[43] S. Tanaka, H. Zakezoe, N. Eber, K. Fodor-Csorba, A. Vajda, A. Buka, *Phys. Rev. E* **2009**, *80*, 021702.

[44] a) D. Wiant, J. T. Gleeson, N. Éber, K. Fodor-Csorba, A. Jákli, T. Tóth-Katona, *Phys. Rev. E* **2005**, *72*, 041712; b) P. Kumar, U. S. Hiremath, C. V. Yelamaggad, A. G. Rossberg, K. S. Krishnamurthy, *J. Phys. Chem. B* **2008**, *112*, 9753; c) P. Kumar, U. S. Hiremath, C. V. Yelamaggad, A. G. Rossberg, K. S. Krishnamurthy, *J. Phys. Chem. B* **2008**, *112*, 9270; d) J. Heuer, R. Stannarius, M.-G. Tamba, W. Weissflog, *Phys. Rev. E* **2008**, *77*, 056206; e) S. Tanaka, S. Dhara, B. K. Sadashiva, Y. Shimbo, Y. Takanishi, F. Araoka, K. Ishikawa, H. Takezoe, *Phys. Rev. E* **2008**, *77*, 041708; f) E. Dorjgotov, K. Fodor-Csorba, J.T. Gleeson, S. Sprunt, A. Jakli, *Liq. Cryst.* **2008**, *35*, 149; g) C. Bailey, K. Fodor-Csorba, J. T. Gleeson, S. Sprunt, A. Jakli, *Soft Matter* **2009**, *5*, 3618; h) S. Kaur, A. belaissaoui, J. W. Goodby, V. Görtz, H.F. Gleeson, *Phys. Rev. E* **2011**, *83*, 041704.

[45] I. Dirking, *Textures of Liquid Crystals*, Wiley-VCH, Weinheim **2003**.

[46] Y. P. Panarin, Y. P. Kalmykov, S.T. Mac Lughadha, H. Xu, J. K. Vij, *Phys. Rev. E* **1994**, *50*, 4763.

[47] a) D. Pociecha, M. Cepic, E. Gorecka, J. Mieczkowski, *Phys. Rev. Lett.* **2003**, *91*, 185501; b) Y. Shimbo, E. Gorecka, D. Pociecha, F. Araoka, M. Goto, Y. Takanishi, K. Ishikawa, J. Meieczkowski, K. Gomola, H. Takezoe, *Phys. Rev. Lett.* **2006**, *97*, 113901; c) Y. Shimbo, Y. Takanishi, K. Ishikawa, E. Gorecka, D. Pociecha, J. Mieczkowski, K. Gomola, H. Takezoe, *Jpn. J. Appl. Phys.* **2006**, *45*, 282; d) K. Gomola, L. Guo, D. Pociecha, F. Araoka, K.Ishikawa, H. Takezoe, *J. Mater. Chem.* **2010**, *20*, 7944; e) L. Guo, K. Gomola, E. Gorecka, D. Pociecha, S. Dhara, F. Araoka, K. Iahikawa, H. Takezoe, *Soft Matter* **2011**, *7*, 2895.

[48] a) C. Keith, M. Prehm, Y. P. Panarin, J. K. Vij, C. Tschierske, *Chem. Commun.* **2010**, *46*, 3702; b) M. Nagaraj, Y. P. Panarin, J. K. Vij, C. Keith, C. Tschierske, *Appl. Phys Lett.* **2010**, *97*, 213505; c) Y. P. Panarin, M. Nagaraj, J. K. Vij, C. Keith, C. Tschierske, *Euro-Phys Lett.* **2010**, *92*, 26002.

[49] a) L. Guo, S. Dhara, B. K. Sadashiva, S. Rasdhika, R. Prathiba, Y. Shimbo, F. Araoka, K. Ishikawa, H. Takezoe, *Phys. Rev. E* **2010**, *81*. 011703; b) M. Gupta, S. Datta, S. Radhika, B. K. Sadashiva, A. Roy, *Soft Matter* **2011**, *7*, 4735.

[50] a) J. Szydlowska, J. Mieczkowski, J. Matraszek, D. W. Bruce, E. Gorecka, D. Pociecha, D. Guillon, *Phys Rev E* **2003**, **67**, 31702; b) C. Keith, R. Amaranatha Reddy, U. Baumeister, C. Tschierske, *J. Am. Chem. Soc.* **2004**, *126*, 14312; c) M. W. Schröder, S. Diele, G. Pelzl, W. Weissflog, *Chem Phys Chem* **2004**, *5*, 99; d) J. P. Bedel, J. C. Rouillon, J. P. Marcerou, H. T. Nguyen, M. F. Achard, *Phys. Rev. E* **2004**, *69*, 61702; e) M. Nakata, R. F. Shao, J. E. Maclennan, W. Weissflog, N. A. Clark, *Phys. Rev. Lett.*, **2006**, *96*, 067801.

[51] a) K. Merkel, A. Kocot, J. K. Vij, G. H. Mehl, T. Meyer, *Phy. Rev. E* **2006**, *73*, 051702; b) L. Tajber, A. Kocot, J. K. Vij, K. Merkel, J. Zalewska-Rejdak, G. H. Mehl, R. Elasser, J. W. Goodby, M. Veith, *Macromolecules* **2002**, *35*, 8601.

[52] a) W. T. Coffey, Yu. P. Kalmykov, *Advances in Liquid Crystals* (Ed: J. K. Vij), Wiley, New York **2000**; b) W. T. Coffey, Yu. P. Kalmykov, *Adv. Chem. Phys.* **2000**, *113*, 487.

[53] This compound was synthesized as a reference compound. Only DSC traces were given for this compound and the values of the phase transition Cr 157 °C SmX 175 °C N_{cybC} 233 °C agree well with the reported DSC curves in ref. [15f]. No attempt was made to synthesize cyclohexanecarboxylates of related 1,3,4-oxadiazoles, as they are known to show much higher melting temperatures.[15f]

[54] The switching current peaks reported for compound **1,3,4-Ox/7**[16a] could not be found for compound **1,3,4-Ox/O8**.

[55] In contrast to $SmAP_R$ phases which occur above a polar $SmAP_A$ phase[48,47e] or a non-polar $B1_{rev}$ phase,[47a–d] no transition to a macroscopic polar order ($SmCP_A$ phase) or formation of layer modulation (B1-type phase) is observed for compounds **C/7** and **D/5** on further cooling the $SmC/SmCP_R$ phase.